Land Long Term Climate Data Record

Vermote et al.

NASA/GSFC

A Land Climate Data Record

Multi instrument/Multi sensor Science Quality Data Records used to quantify trends and changes

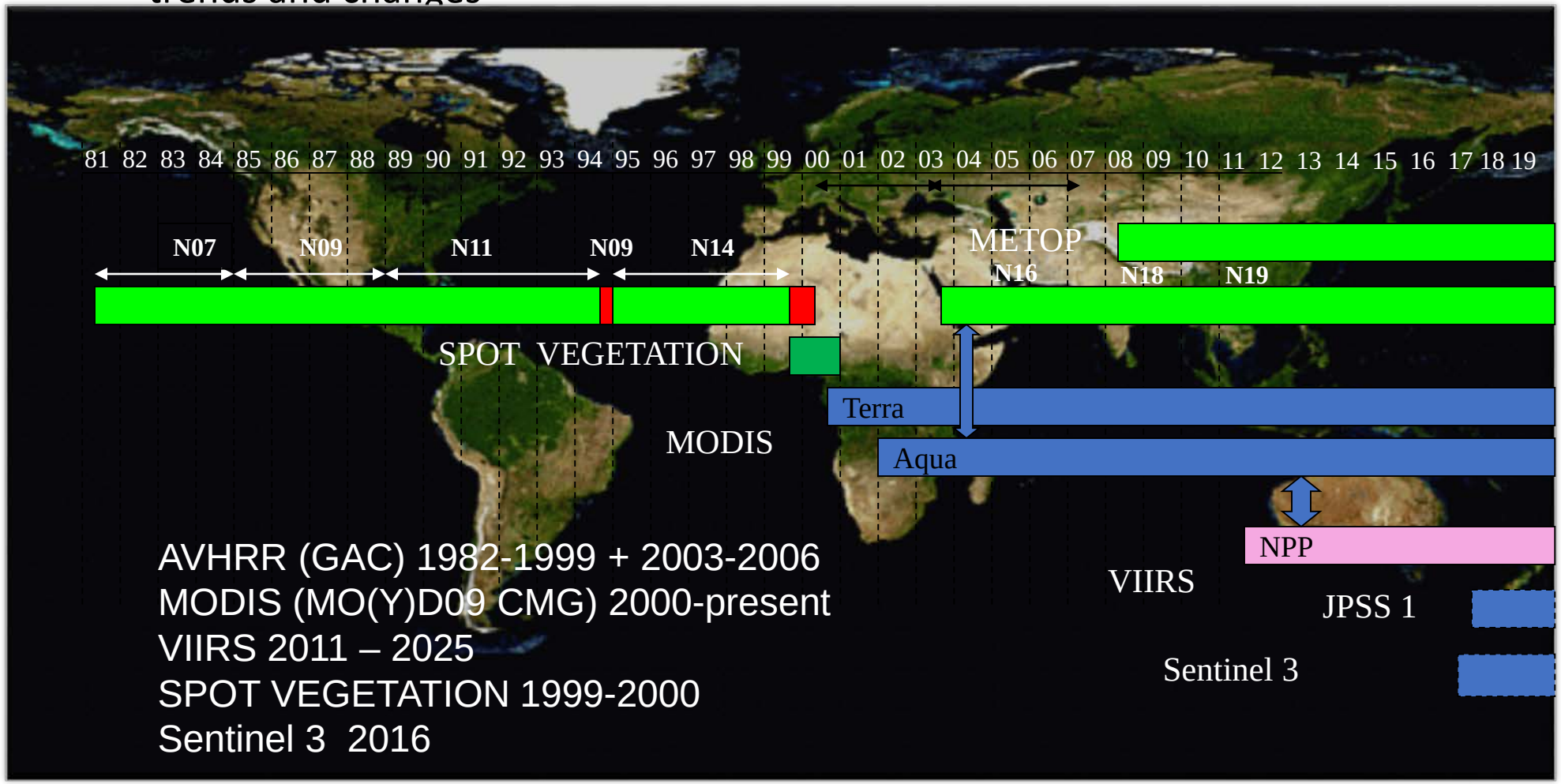

Emphasis on data consistency – characterization rather than degrading/smoothing the data

Land Climate Data Record (Approach)

Needs to address geolocation, calibration, atmospheric/BRDF correction issues

CALIBRATION

Degradation in channel 1
(from Ocean observations)

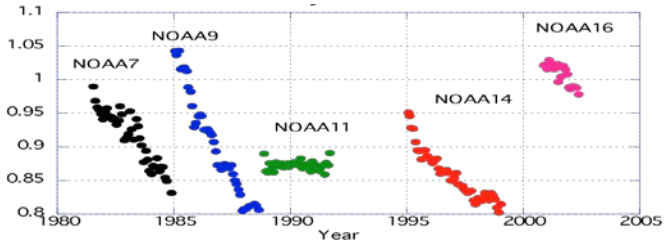

ATMOSPHERIC CORRECTION

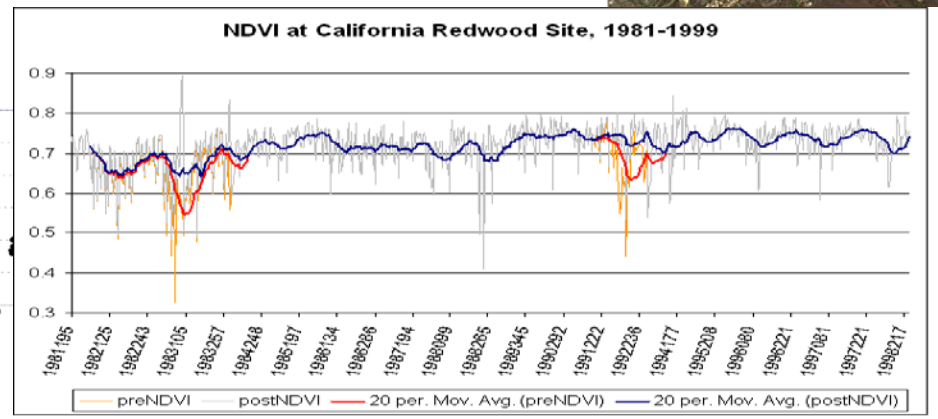

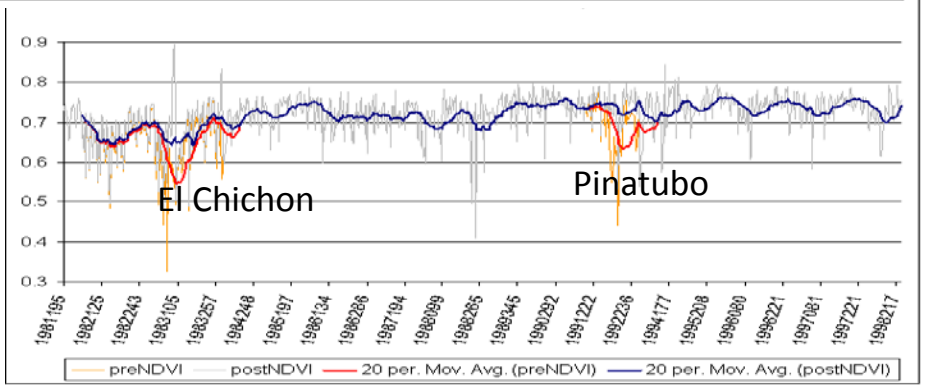

BRDF CORRECTION

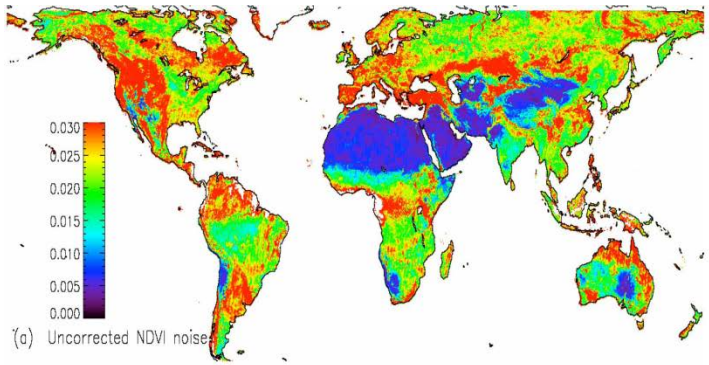

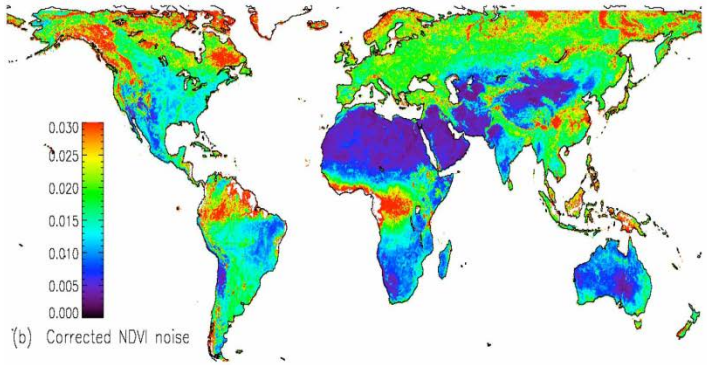

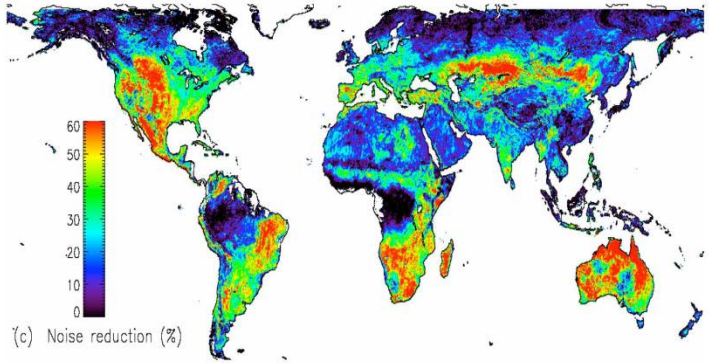

Atmospheric correction (AC)

- Estimate of the **surface spectral reflectance**, as would have been measured at ground level if there were **no atmospheric scattering or absorption**
- Generic approach for AC for multiple sensors
- AC products for EO sensors:
  - MODIS (Terra, Aqua)
    - Products: MOD09, MYD09
  - VIIRS (S-NPP)
    - Products: VNP09
  - OLI (Landsat-8) and MSI (Sentinel-2)
    - LaSRC algorithm/product
    - Harmonization Landsat / Sentinel 2 (HLS) project
    - USGS' on demand SR product for OLI

(Vermote et al., 2016, *RSE*)

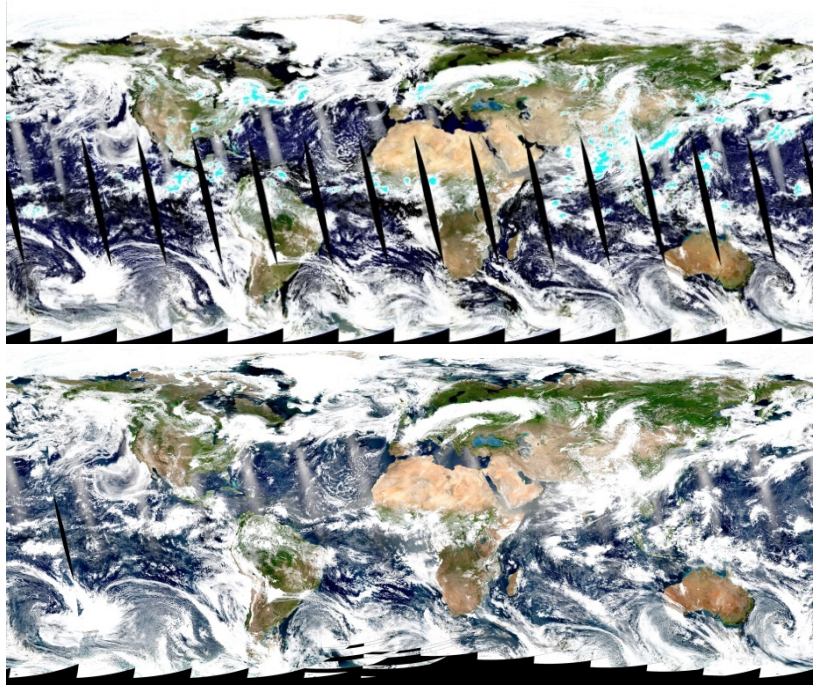

A true color composite of MODIS/Aqua (*top*) and VIIRS/S-NPP (*bottom*) images acquired on July, 1, 2017

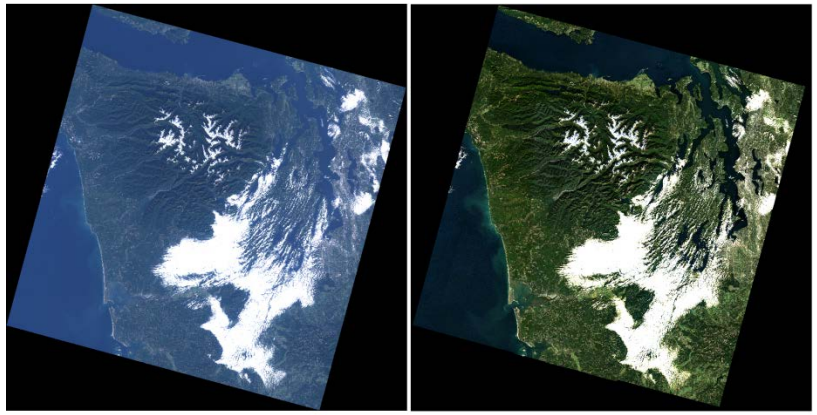

A true color composite of Landsat-8 image without AC (*left*) and with AC (*right*). Image is acquired on October, 14, 2013

Flowchart of the LaSRC atmospheric correction scheme

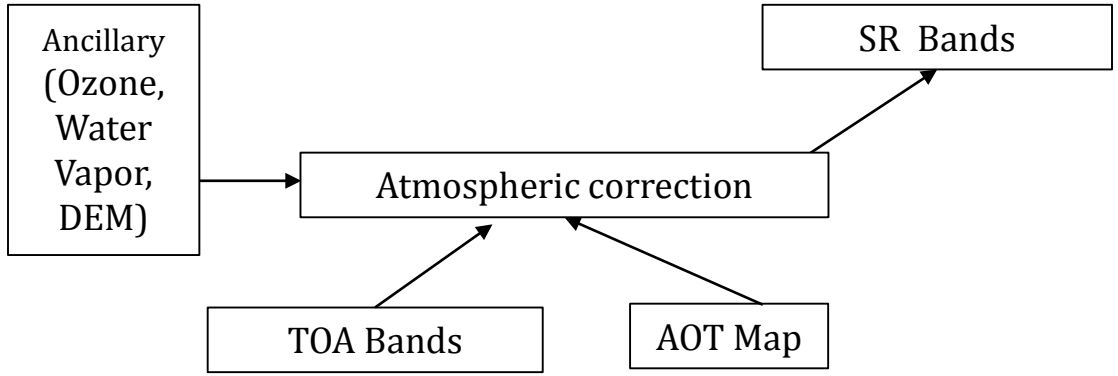

LaSRC Surface Reflectance

LaSRC relies on

- **the use of very accurate (better than 1%) vector radiative transfer modeling of the coupled atmosphere-surface system (6S)**
- the inversion of key atmospheric parameters
  - Aerosols
  - ***Water vapor and ozone from daily MODIS product.***

Home page: http://modis-sr.ltdri.org

AVHRR CALIBRATION

INT. J. REMOTE SENSING, 1995, VOL. 16, NO. 13, 2317–2340

Absolute calibration of AVHRR visible and near-infrared channels using ocean and cloud views

E. VERMOTE
Laboratory for Global Remote Sensing, Lefrak Hall, University of Maryland, College Park Maryland, U.S.A.

and Y. J. KAUFMAN
Laboratory for Atmospheres Code 913, NASA GSFC, Greenbelt MD 20771, U.S.A.

(Received 8 February 1994; in final form 21 August 1994)

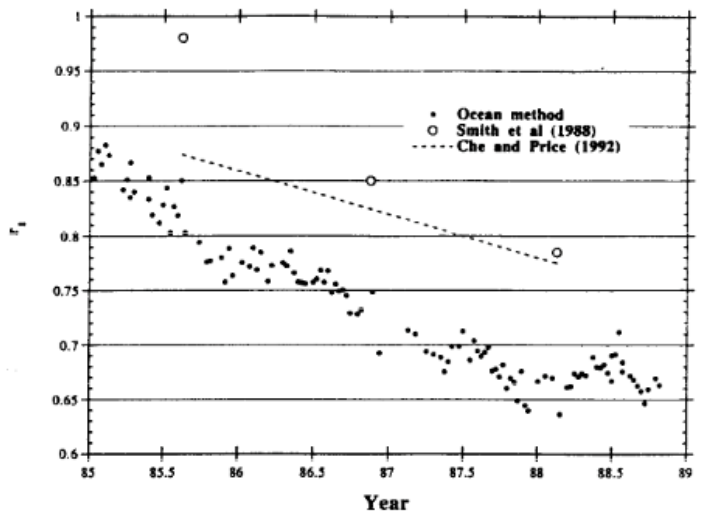

(a)

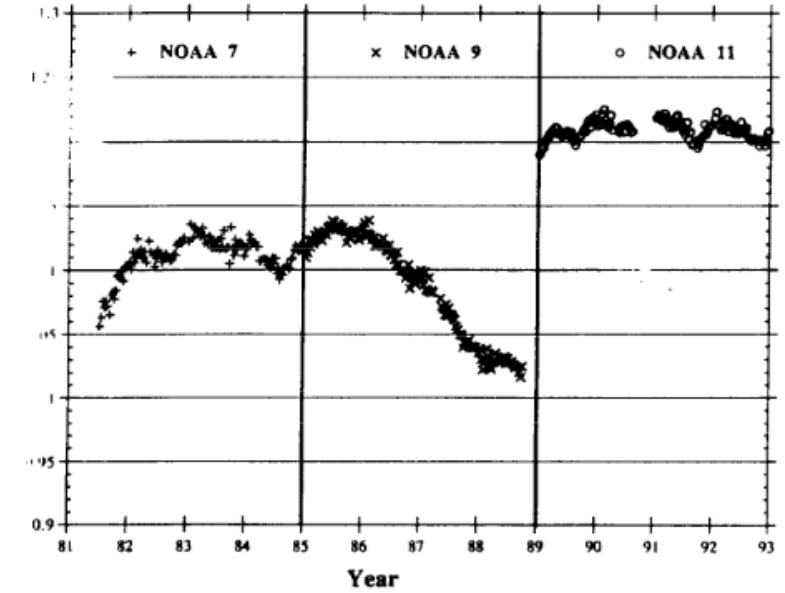

Ratio between the deterioration of channels 1 and 2, r_{12} as observed over high reflective clouds for NOAA-7, -9, -11.

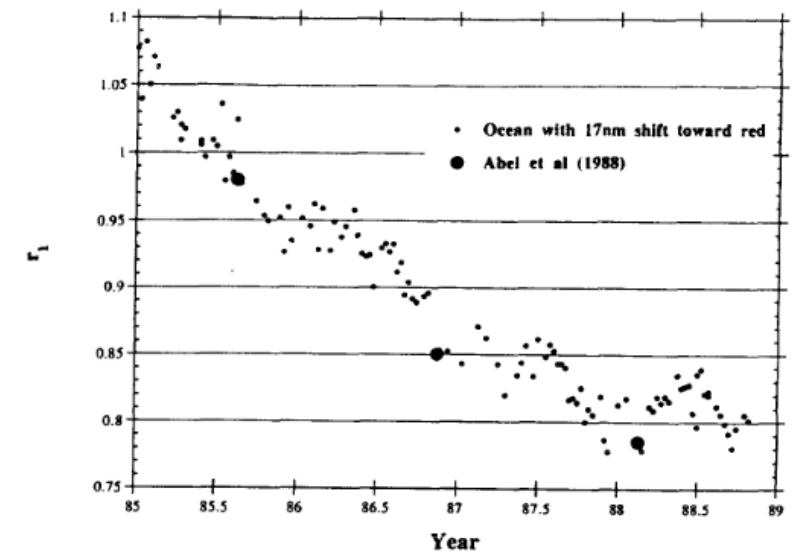

(a)

AVHRR CALIBRATION

Calibration of NOAA16 AVHRR over a desert site using MODIS data

E.F. Vermote [a,*], N.Z. Saleous [b]

[a] University of Maryland, Department of geography and NASA GSFC Code 614.5, United States
[b] SAIC and NASA GSFC Code 614.5, United States

Received 24 February 2006; received in revised form 16 June 2006; accepted 27 June 2006

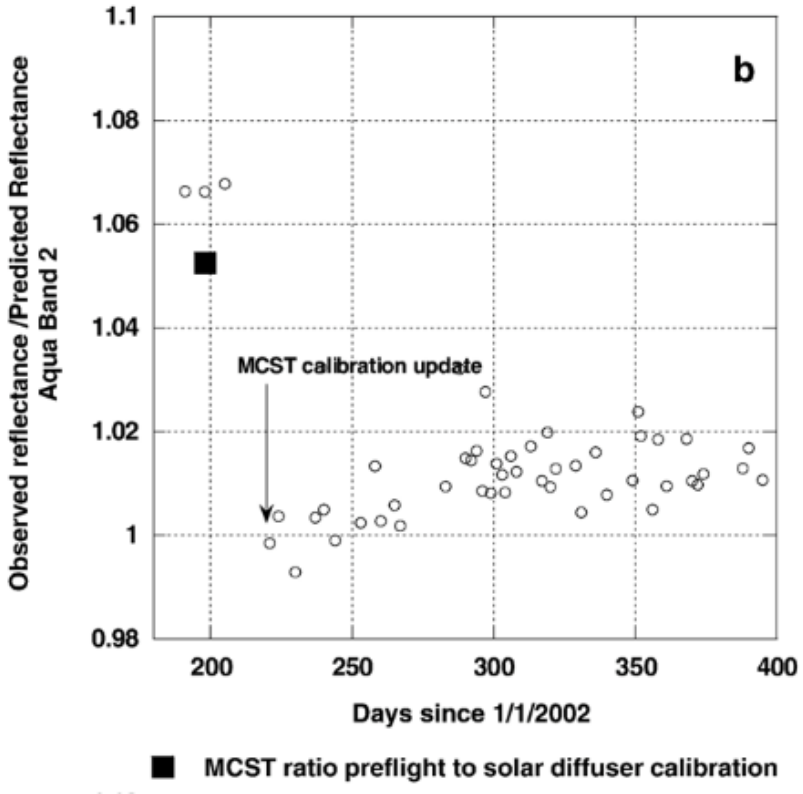

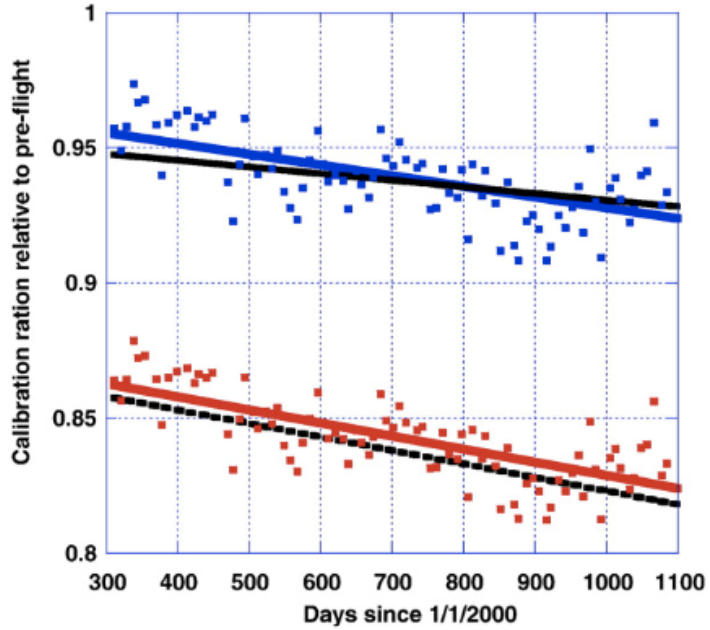

Fig. 11. Comparison of the desert calibration trends for band 1 (black solid line) and band 2 (black interrupted line), with the trends obtained using the Ocean and Clouds method (Vermote and Kaufman, 1995) for band 1 (blue line and square) and band 2 (red line and square).

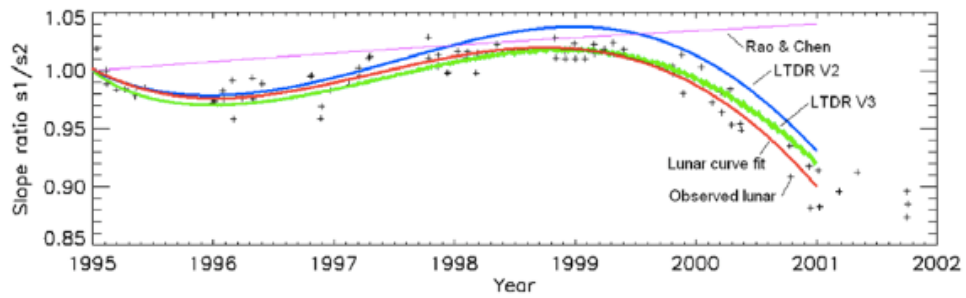

Figure 3. Comparison of the long-term trend of slope ratio for NOAA 14 between lunar, LTDR, and NOAA operational (red, lunar curve fit; pluses, lunar observation; green, LTDR version 3; blue, LTDR version 2; and pink, NOAA operational).

AVHRR CALIBRATION

A 30+ Year AVHRR Land Surface Reflectance Climate Data Record and Its Application to Wheat Yield Monitoring

Belen Franch [1,2,*], Eric F. Vermote [2], Jean-Claude Roger [1,2], Emilie Murphy [1,2], Inbal Becker-Reshef [1], Chris Justice [1], Martin Claverie [1,2], Jyoteshwar Nagol [1], Ivan Csiszar [3], Dave Meyer [4], Frederic Baret [5], Edward Masuoka [2], Robert Wolfe [2] and Sadashiva Devadiga [6]

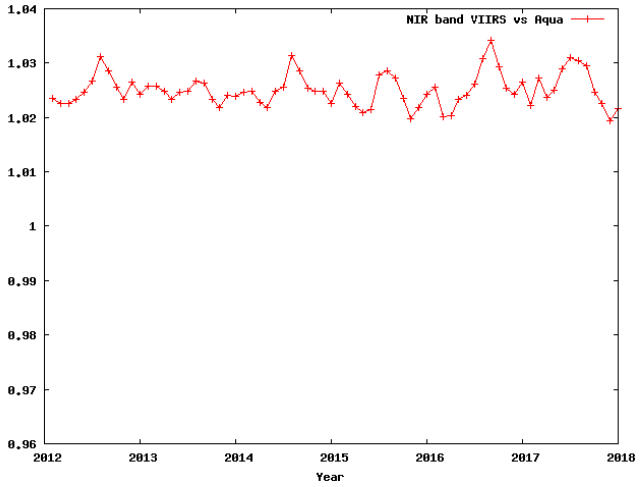

BELMANIP sites

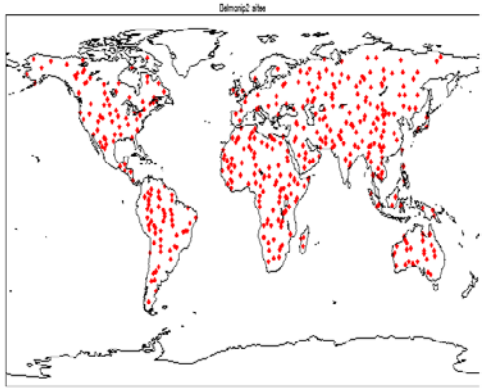

Automated monthly VIIRS cross comparison (over BELMANIP sites) with MODIS Aqua from 2012. the stability of both VIIRS and MODIS Aqua is excellent in both red and NIR as shown (+/- 0.5%).

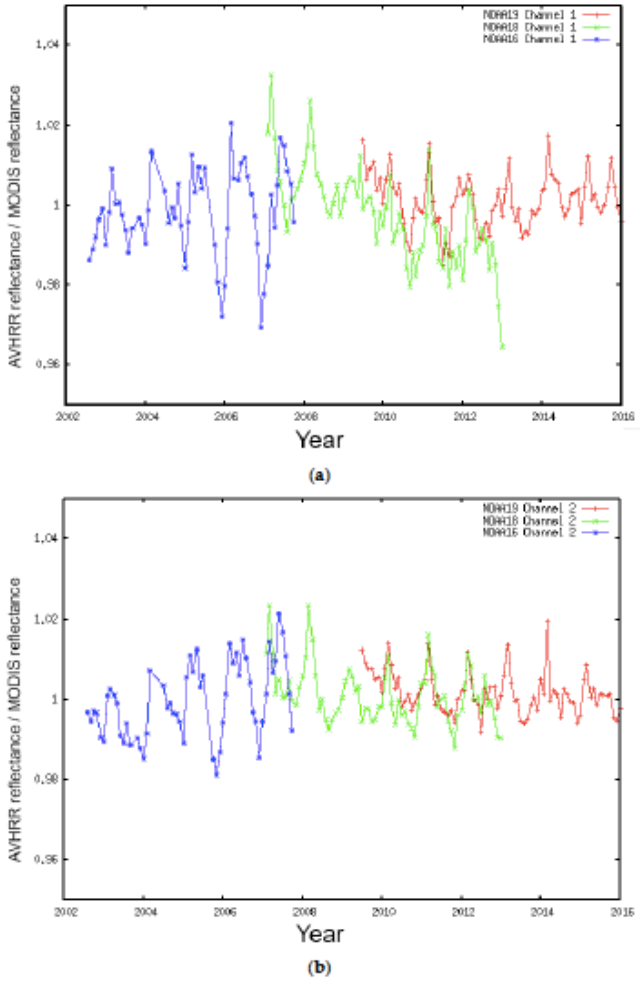

Figure 7. Cross-comparison between AVHRR N16, N18, and N19 and MODIS Terra ratios for the BELMANIP2 sites for the red band (**a**) and the near infrared band (**b**).

AVHRR GEOLOCATION

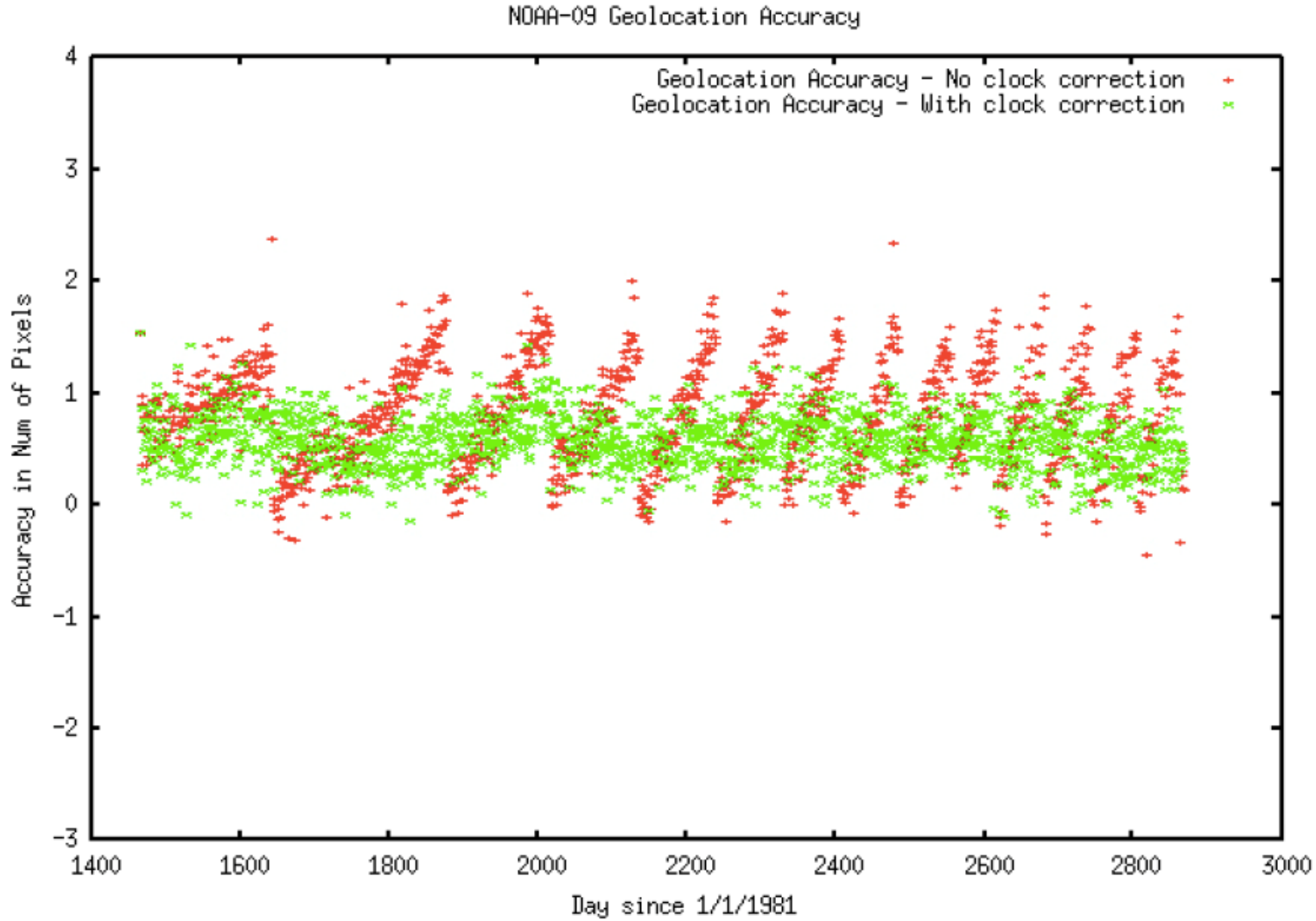

Figure 2. Accuracy assessment of the geolocation of AVHRR products using the coastal chips database (in fraction of pixels). Green is with clock correction, and red is without clock correction.

AVHRR CLOUD SCREENING FROM CLAVR (1996) till now

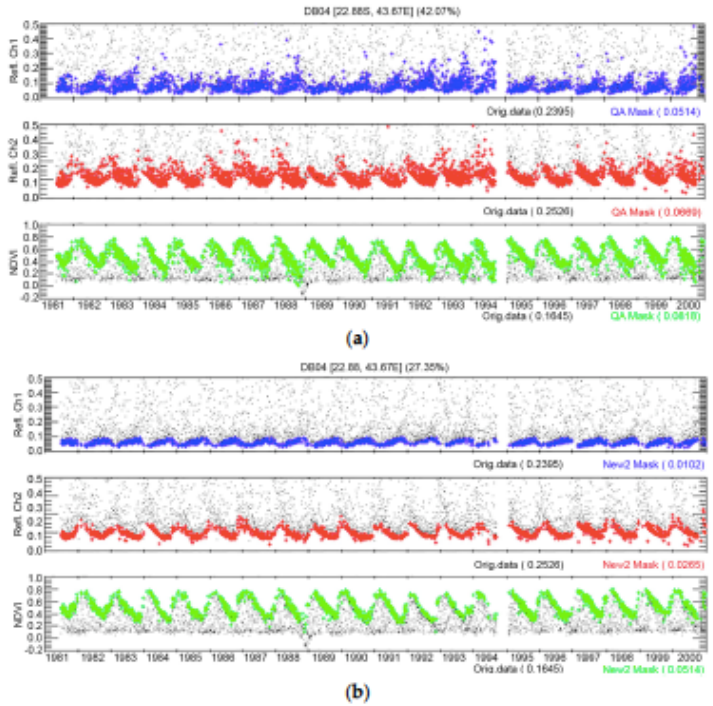

Figure 5. AVHRR time-series of channel 1 (blue) and channel 2 (red) surface reflectance and the NDVI (green) using (**a**) CLAVR or (**b**) LCDR cloud masks for a deciduous broadleaf site in Madagascar. Black symbols are clouds. The standard deviation of the unfiltered data of the time series (original data) and of the cloud filtered time series (QA mask for CLAVR, New2 mask for the LCDR cloud mask) are also provided for each of the bands and the NDVI. The percentage of clear data is also provided for each cloud mask at the top of the figure.

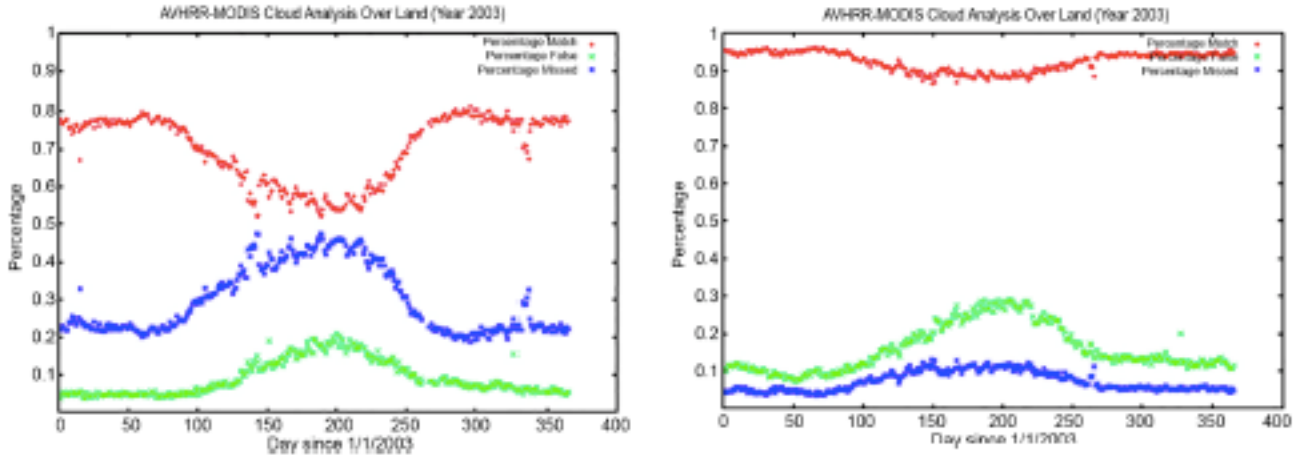

Figure 4. Evaluation of the global performance of the current cloud mask for NOAA16-AVHRR versus the MODIS Aqua cloud mask. Results are reported as percentages. The left side is the CLAVR algorithm [14]. The right side is the current LCDR improved cloud mask. The MODIS Aqua cloud mask is used as truth in this comparison. Red symbols (match) show the percentage of agreement between AVHRR and MODIS, Green symbols (false) show the percentage of cases where AVHRR erroneously detects clouds. Blue symbols (missed) show the percentage of cases where AVHRR missed clouds.

AVHRR THE URGE FOR ATMOSPHERIC CORRECTION

Mount Pinatubo eruption 1991 second largest in 20h century

Stratospheric AOT from AVHRR

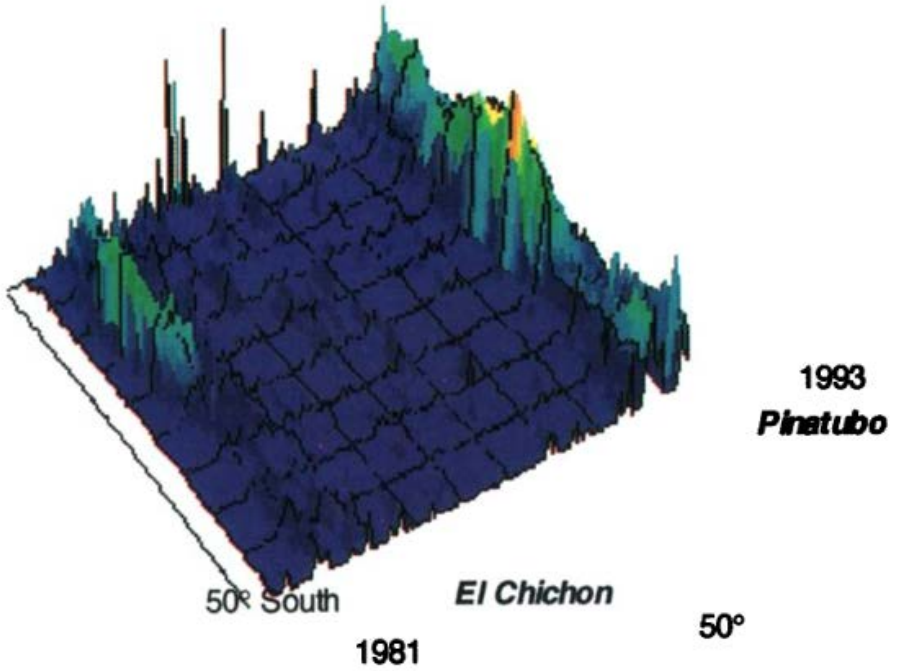

Plate 2. Monthly average of the stratospheric aerosol optical depth deduced from the advanced very high resolution radiometer (AVHRR) data showing major eruptions of El Chichon (1982) and Pinatubo (1991).

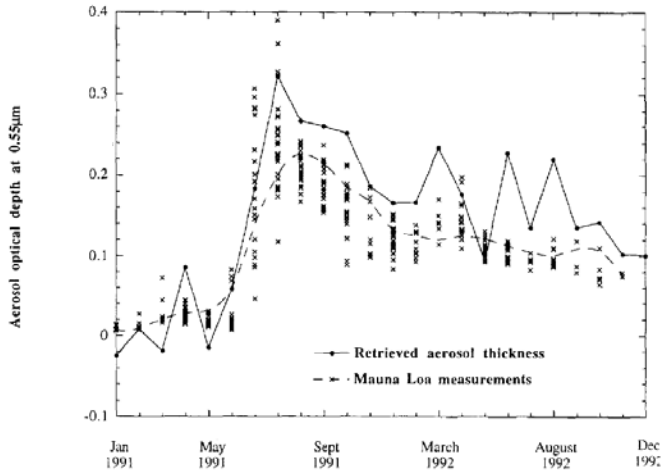

FIGURE 4 Comparison between retrieved "stratospheric" optical thickness and measurements taken at Manua Loa observatory

Vermote, E., Saleous, N.E., Kaufman, Y.J. and Dutton, E., 1997. Data pre-processing: Stratospheric aerosol perturbing effect on the remote sensing of vegetation: Correction method for the composite NDVI after the Pinatubo eruption. Remote Sensing Reviews, 15(1-4), pp.7-21.

El Chichon and Pinatubo

Comparison of the Stratospheric AOT obtained from AVHRR with SAGE data for September 1982 (El Chichon eruption)

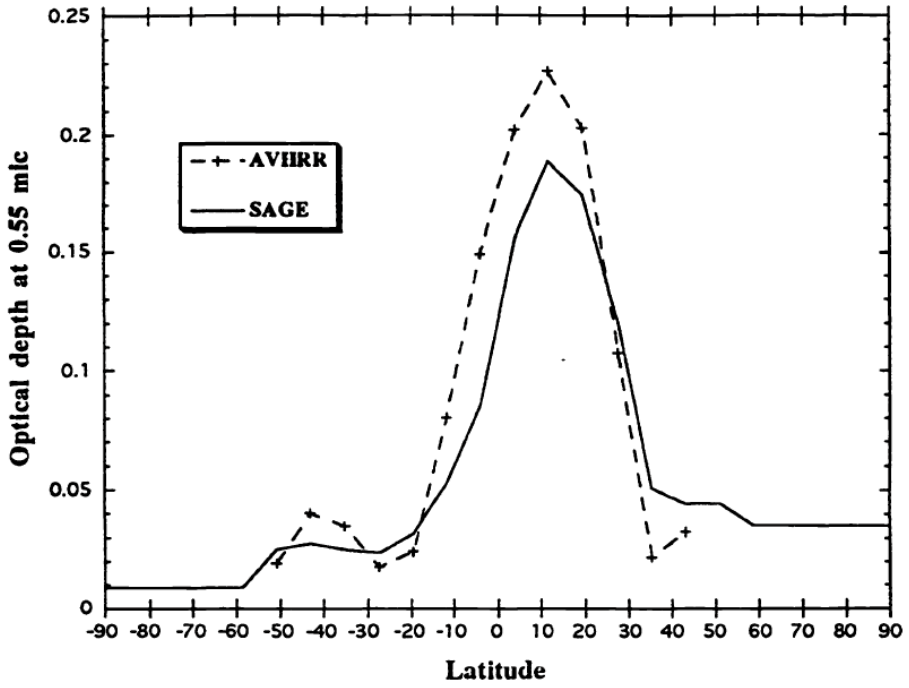

Figure 6: Latitudinal "stratospheric" profile observed after Mt. Pinatubo eruption.

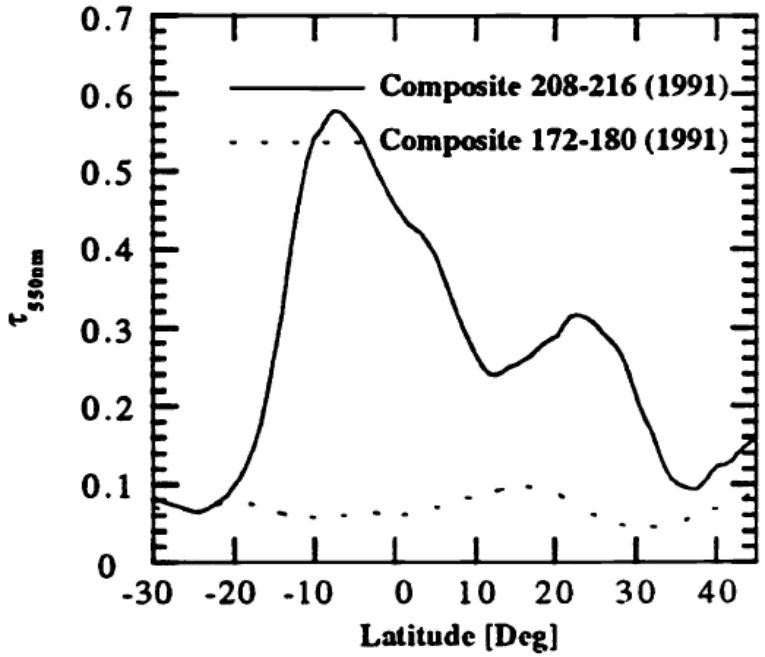

Eric F. Vermote, Nazmi El Saleous, "Stratospheric aerosol perturbing effect on the remote sensing of vegetation: operational method for the correction of AVHRR composite NDVI," Proc. SPIE 2311, Atmospheric Sensing and Modelling, (4 January 1995);

AVHRR long term correction for stratospheric aerosol has been successfully tested.

Red curve: AVHRR NDVI not corrected for stratospheric aerosol
Blue curve: AVHRR NDVI corrected for stratospheric aerosol

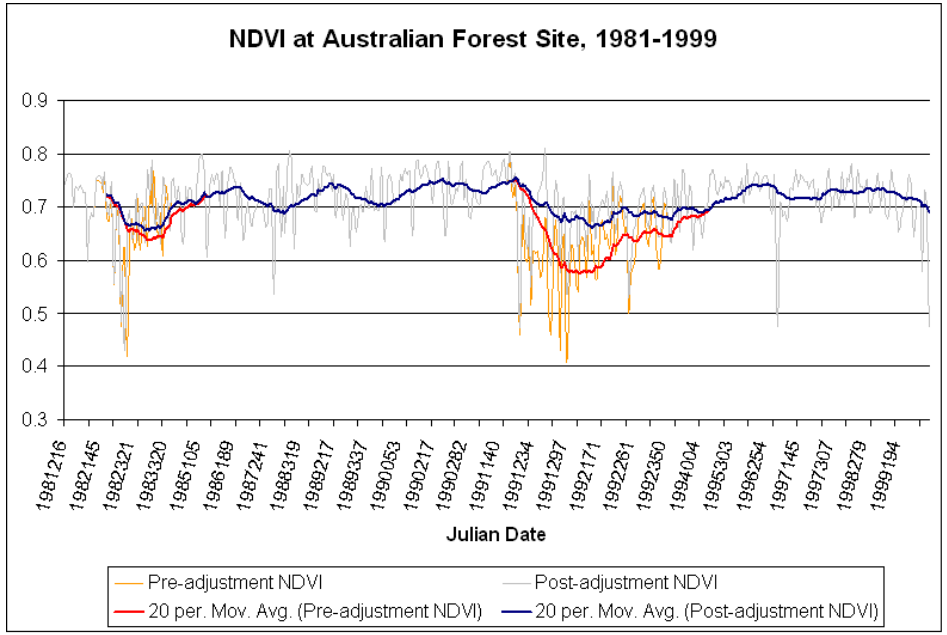

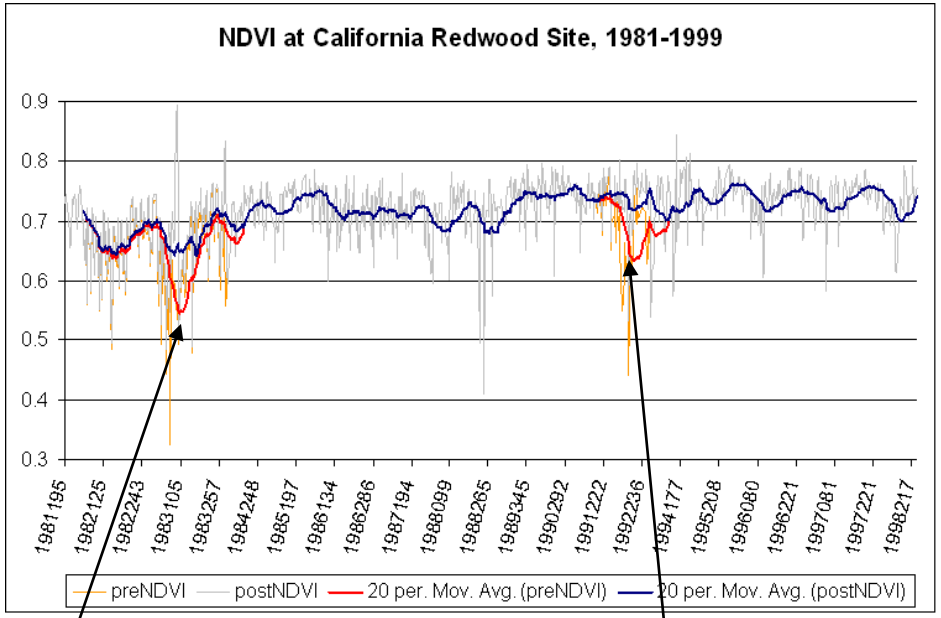

El Chichon

Pinatubo

AVHRR **ATMOSPHERIC** CORRECTION EVOLUTION

Pathfinder I: Partial correction
James, M.E. and Kalluri, S.N., 1994. The Pathfinder AVHRR land data set: An improved coarse resolution data set for terrestrial monitoring. *International Journal of Remote Sensing*, *15*(17), pp.3347-3363.

Pathfinder II: Improved correction fixed Pathfinder I issues
El Saleous, N.Z., Vermote, E.F., Justice, C.O., Townshend, J.R.G., Tucker, C.J. and Goward, S.N., 2000. Improvements in the global biospheric record from the Advanced Very High Resolution Radiometer (AVHRR). *International Journal of Remote Sensing*, *21*(6-7), pp.1251-1277.

LTDR (Version 2.,3., 4.): Improvement on going, water vapor correction, aerosol correction.
Franch, B., Vermote, E., Roger, J.C., Murphy, E., Becker-Reshef, I., Justice, C., Claverie, M., Nagol, J., Csiszar, I., Meyer, D. and Baret, F., 2017. A 30+ year AVHRR land surface reflectance climate data record and its application to wheat yield monitoring. *Remote Sensing*, *9*(3), p.296

AVHRR ATMOSPHERIC CORRECTION EVOLUTION

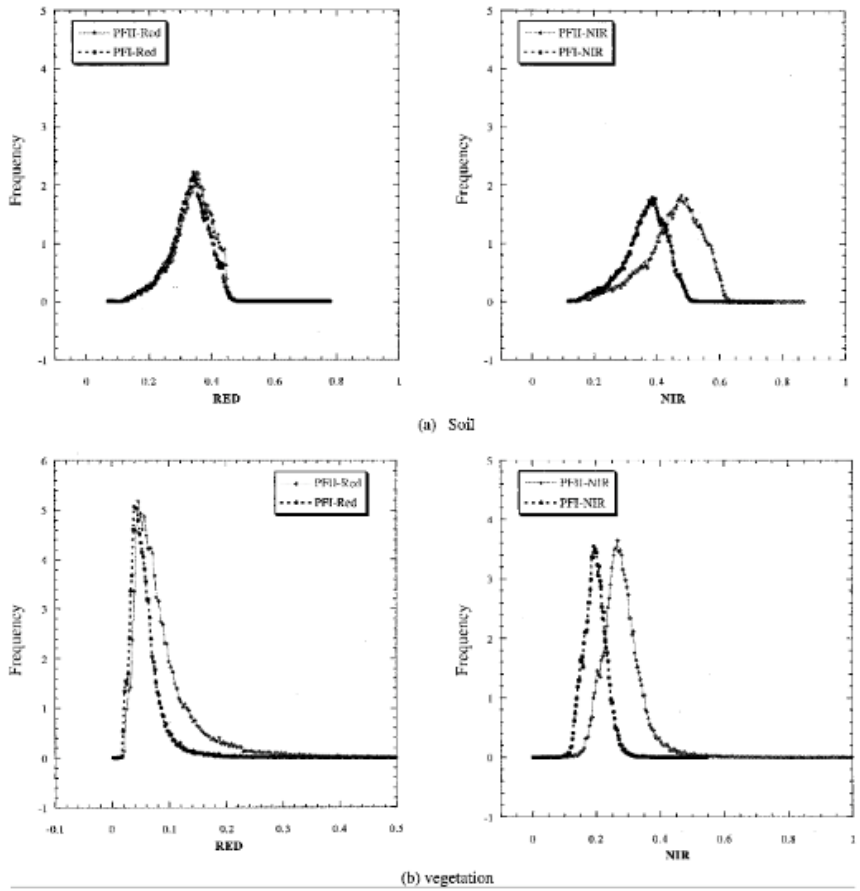

Figure 15. Red and near-infrared reflectance histograms computed from 10-day composites from AVHRR Land Pathfinder II (PFII) and AVHRR Pathfinder I (PFI) data sets for soil (*a*) and vegetation (*b*).

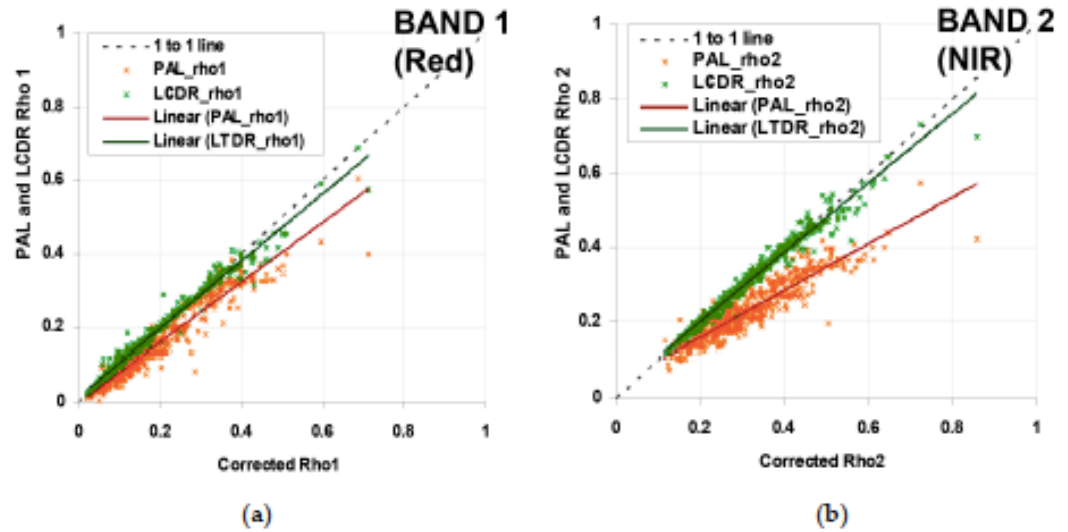

Figure 6. Comparison of current AVHHR Surface Reflectance (LCDR) and PAL data for channel 1 (**a**) and channel 2 (**b**) at 48 AERONET sites for 1999 (from [9]). The *x*-axis shows the surface reflectance values determined from the 6S code supplied with atmospheric parameters from an AERONET sun photometer, while the *y*-axis shows the surface reflectances retrieved from the AVHRR data using current LCDR and PAL algorithms.

AVHRR LTDR IMPROVEMENTS ARE ON GOING

Villaescusa-Nadal, J.L., Franch, B., Roger, J.C., Vermote, E.F., Skakun, S. and Justice, C., 2019. Spectral Adjustment Model's Analysis and Application to Remote Sensing Data. *IEEE Journal of Selected Topics in Applied Earth Observations and Remote Sensing*.

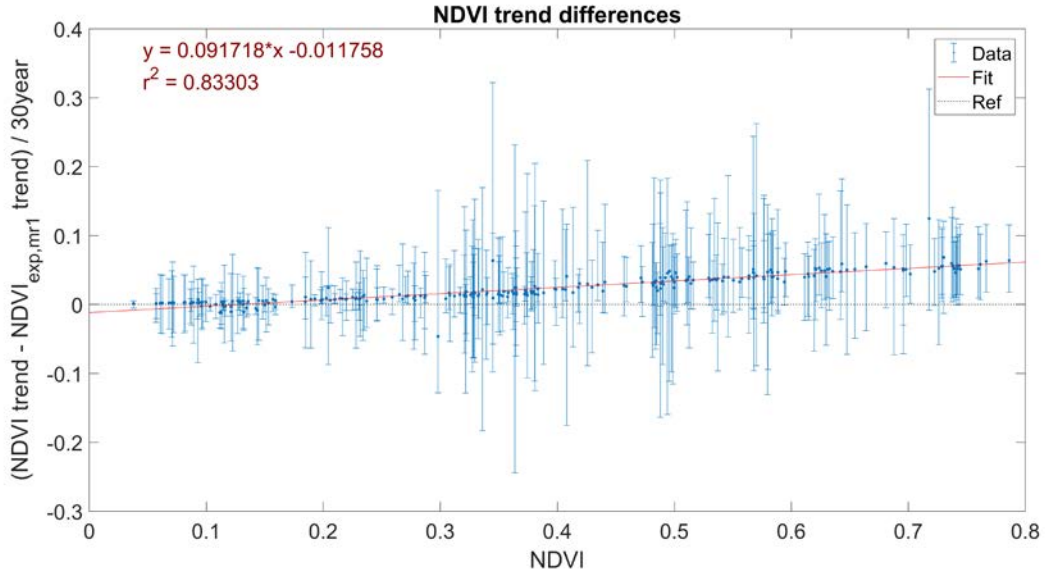

AVHRR LTDR IMPROVEMENTS ARE ON GOING

Villaescusa-Nadal, J.L., Franch, B., Vermote, E.F. and Roger, J.C., 2019. Improving the AVHRR Long Term Data Record BRDF Correction. *Remote Sensing*, *11*(5), p.502.

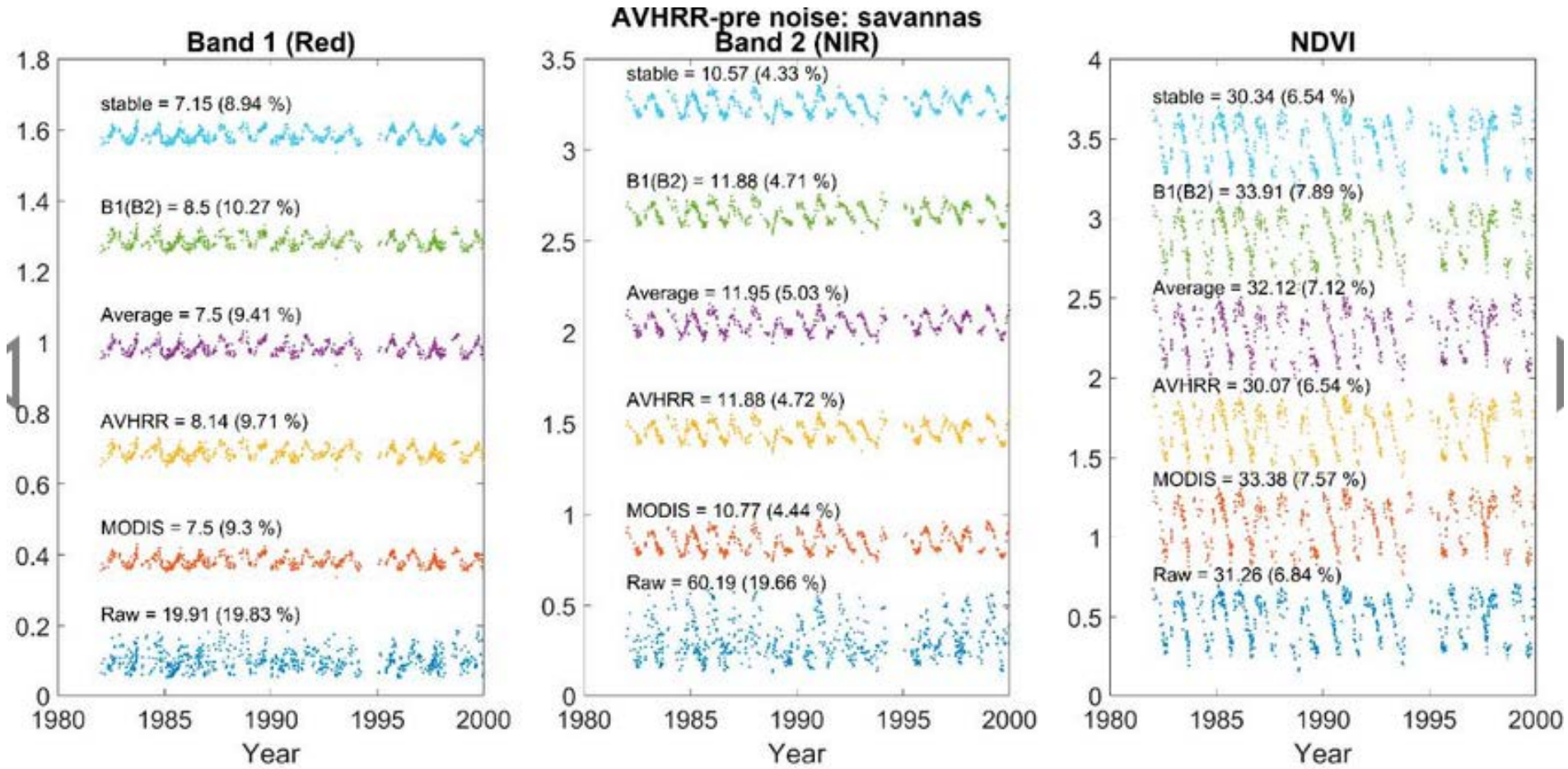

AVHRR LTDR APPLICATIONS

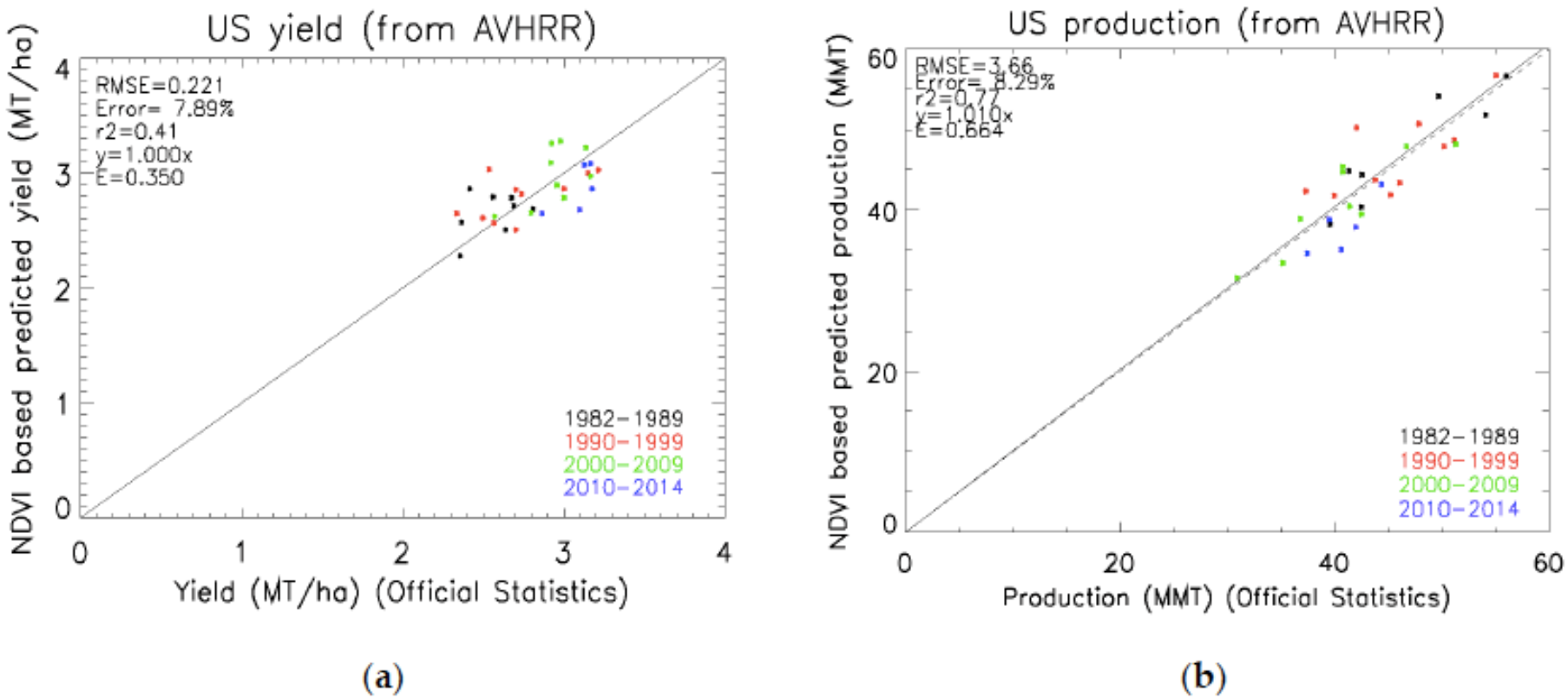

Figure 9. National winter wheat predicted yield (**a**) and production (**b**) in the U.S., applying the 'original' method [1] to AVHRR data plotted against USDA-reported statistics (https://quickstats.nass.usda.gov).

AVHRR LTDR APPLICATIONS

nature
International journal of science

Letter | Published: 08 August 2018

Global land change from 1982 to 2016

Xiao-Peng Song, Matthew C. Hansen, Stephen V. Stehman, Peter V. Potapov, Alexandra Tyukavina, Eric F. Vermote & John R. Townshend

Here we analyse 35 years' worth of satellite data and provide a comprehensive record of global land-change dynamics during the period 1982–2016. We show that—contrary to the prevailing view that forest area has declined globally[5]—tree cover has increased by 2.24 million km^2 (+7.1% relative to the 1982 level). This overall net gain is the result of a net loss in the tropics being outweighed by a net gain in the extratropics.

Extended Data Table 1 Estimates of 1982 land-cover area and 1982–2016 land-cover change at continental and global scales

From: Global land change from 1982 to 2016

Continent	Tree canopy cover								Short vegetation cover								Bare ground cover							
		Annual net change				Gross change			Annual net change				Gross change			Annual net change				Gross change		
	Area 1982 (10^3 km^2)	Slope (10^3 km^2 yr^{-1})	Lower (10^3 km^2 yr^{-1})	Upper (10^3 km^2 yr^{-1})	p	loss (10^3 km^2)	gain (10^3 km^2)	Area 1982 (10^3 km^2)	Slope (10^3 km^2 yr^{-1})	Lower (10^3 km^2 yr^{-1})	Upper (10^3 km^2 yr^{-1})	p	loss (10^3 km^2)	gain (10^3 km^2)	Area 1982 (10^3 km^2)	Slope (10^3 km^2 yr^{-1})	Lower (10^3 km^2 yr^{-1})	Upper (10^3 km^2 yr^{-1})	p	loss (10^3 km^2)	gain (10^3 km^2)
Africa	4672	-1.9	-7.6	3.6	0.609	-267	262	11653	14.8	6.5	23.2	0.016	-268	571	13413	-12.4	-19.9	-4.7	0.020	-371	105
Asia	8457	37.5	28.0	45.3	0.000	-178	1170	21774	-22.9	-34.5	-9.6	0.008	-1261	760	13926	-15.1	-23.1	-7.4	0.002	-798	358
Europe	2719	28.3	20.4	32.8	0.000	-17	758	6320	-22.0	-27.3	-14.7	0.000	-673	50	668	-4.3	-5.8	-2.6	0.000	-92	9
North America	5815	15.6	3.5	24.2	0.020	-205	583	12921	-12.7	-4.1	-2.2	0.031	-594	286	4847	-2.5	-7.3	2.2	0.363	-186	140
South America	8767	-14.1	-20.5	-7.4	0.001	-621	190	7165	14.8	8.1	21.0	0.002	-224	655	1717	1.9	-1.2	3.8	0.307	-92	102
Oceania	680	0.1	-1.4	1.7	0.887	-40	56	4600	-4.4	-12.1	3.4	0.349	-132	50	2772	5.2	-3.9	12.5	0.280	-35	113
Global	31628	66.0	27.3	100.5	0.008	-1331	3039	64539	-26.0	-64.8	15.2	0.244	-3170	2380	37412	-34.0	-52.3	-10.0	0.023	-1582	830

Annual net change in land cover (slope) and 1982 land-cover area were estimated using Theil–Sen regression of the time series of annual land-cover area per continent or over the globe (excluding Antarctica). Lower and upper slopes represent the 90% confidence interval. Reported P value is for the two-sided Mann–Kendall test for trend, with $P < 0.05$ used to define statistical significance, and a sample size of $n = 35$ years. Gross change in land cover was estimated on the basis of per-pixel non-parametric trend analysis. Per-pixel loss and gain were summed to derive gross loss and gain at the aggregated scales.

CONCLUSIONS

- AVHRR data record is well alive and continue to improve and be used by a large land user community.

- Most of the improvement are due to the overlapping with MODIS Aqua, Terra.

- We recommend operating missions as long as possible to enable overlap of at least a few years (especially for applications)